The use of the tertiary alkyl tetraoxide–peroxyl equilibrium, ROOOOR ⇌ 2RO$_2^{\bullet}$, as a clean source of tertiary alkyl peroxyls †

James D. Honeywill and Brynmor Mile

School of Chemistry, University of Bristol, Cantock's Close, Bristol, UK BS8 1TS

Received (in Cambridge, UK) 27th September 2001, Accepted 30th November 2001
First published as an Advance Article on the web 21st January 2002

Below 155 K there is a dynamic equilibrium between tertiary alkylperoxyls and their tetraoxide ‡ combination products. The system can be recycled repeatedly between 113 and 155 K without loss of radicals. The stationary peroxyl concentration depends solely on the temperature and the initial tetraoxide level. The equilibrium provides a clean source of peroxyls, since no other radicals such as alkoxyls are present. We have used the equilibrium to determine the mechanisms, and to estimate the rate constants for the reactions of tertiary alkylperoxyls with antioxidant and spin trap substrates. The method depends on rapidly mixing cold solutions of the substrates and solutions containing equilibrium concentrations of tertiary peroxyls. The mixing takes place *in situ* within an EPR cavity and the decay of the peroxyl signal is monitored continuously by EPR. The decay profiles have been kinetically analysed at three levels of approximation with the most accurate rate parameters being obtained by kinetic modelling of the total reaction scheme.The rate parameters for the reaction of peroxyls and the antioxidant, IONOL, are in good agreement with those determined by other kinetic EPR methods (KEPR). Studies of the reaction with the much used spin trap DMPO have shown that a rapid removal of peroxyls does not result in a paramagnetic mono-radical spin adduct, but yields a diamagnetic product probably containing two peroxyls added sequentially or concertedly to the spin trap.

Introduction

In the early 1960's kinetic, isotopic and product studies[1–5] suggested that alkyl polyoxide species could exist as stable molecules and were not merely transients or transition complexes. Using additivity relationships, Benson and Buss[6,7] calculated that alkyl tetraoxides would be stable only below 100 K, and alkyl trioxides below 250 K.

Bartlett and Guaraldi[8] provided the first experimental evidence for persistent alkyl tetraoxides. They showed that both di-*tert*-butyl tetraoxide and di-*tert*-butyl trioxides could be prepared at low temperatures and that they were in equilibrium with their respective oxyl radicals.

$$\mathrm{ROOOOR} \rightleftharpoons 2\mathrm{ROO}^{\bullet} \quad (1)$$

$$\mathrm{ROOOR} \rightleftharpoons \mathrm{ROO}^{\bullet} + \mathrm{RO}^{\bullet} \quad (2)$$

The chemistry of tetraoxides is now well established and the thermodynamic parameters for many alkyl tetraoxide–peroxyl equilibria have been measured.[9–11] At temperatures below 155 K the di-*tert*-alkyl tetraoxides are in equilibrium with their parent *tert*-alkylperoxyls at concentrations determined by the equilibrium constant, $K = k_1/k_{-1}$. The complete reversibility of the forward and back reactions below 155 K enables the tertiary peroxyl concentration to be recycled indefinitely between small levels at low temperature to high levels, corresponding to almost complete dissociation, above 155 K. (It is worth noting that primary and secondary alkyl tetraoxides are far less stable and the corresponding peroxyl concentrations cannot be recycled in this way.)

This equilibrium could provide a clean source of tertiary peroxyls for studies of their reactions with substrates such as antioxidants and spin traps. A potential advantage is that no other radicals, such as alkoxyls, will be present, so simplifying mechanistic and kinetic interpretations of results.

$$^{t}\mathrm{BuO_2}^{\bullet} + {}^{t}\mathrm{BuO_2}^{\bullet} \underset{k_{-1}}{\overset{k_1}{\rightleftharpoons}} {}^{t}\mathrm{BuO_4Bu^t} \quad (3)$$

$$[{}^{t}\mathrm{BuO_2}^{\bullet}] = \left\{\frac{[{}^{t}\mathrm{BuO_4Bu^t}]}{K}\right\}^{\frac{1}{2}} \quad (4)$$

Here we report an examination of the use of this potentially clean source of tertiary peroxyls. Our approach was to establish a stable concentration of $^{t}RO_2^{\bullet}$ in equilibrium with the corresponding tetraoxide and then to rapidly add a known concentration of a reactive substrate. The decrease of [$^{t}RO_2^{\bullet}$] with time after substrate addition should yield the rate constant for the reaction with $^{t}RO_2^{\bullet}$ [reactions (5) and (6)]. The reactions were

$$\mathrm{RO_2}^{\bullet} + \mathrm{AH} \longrightarrow \mathrm{ROOH} + \mathrm{A}^{\bullet}\ (\mathrm{AH} = \text{Phenolic antioxidant}) \quad (5)$$

$$\mathrm{RO_2}^{\bullet} + \mathrm{ST} \longrightarrow \mathrm{ROOST}^{\bullet}\ (\mathrm{ST} = \text{Spin trap}) \quad (6)$$

carried out *in situ* in an electron paramagnetic resonance (EPR) cavity held at a prescribed temperature thus enabling the decay of $^{t}RO_2^{\bullet}$ to be monitored continuously by EPR. Our use of the tetraoxide equilibrium to establish the identity of oxyl radicals trapped by the DMPO spin trap has already been briefly described.[12]

Experimental

All EPR measurements were made at X band on a Varian E109 spectrometer with 100 kHz modulation and phase sensitive detection at this frequency. An Oxford low temperature unit enabled the temperature of the EPR cavity to be varied from 110 K to ambient.

† Electronic supplementary information (ESI) available: second level approximation. See http://www.rsc.org/suppdata/p2/b1/b108805j/
‡ In this article, tetraoxide indicates a derivative of tetraoxidane.

DOI: 10.1039/b108805j

Preparation of tertiary alkyl tetraoxides

tert-Alkyl tetraoxides were prepared by photolysing di-*tert*-butyl peroxide (DTBP) solutions (10^{-5} M) in oxygenated 2-methylbutane (2MB) at low temperatures with a medium pressure mercury xenon lamp [reactions (7)–(10)].

$$^{t}BuOOBu^{t} + h\nu \longrightarrow 2\,^{t}BuO^{\bullet} \quad (7)$$

$$^{t}BuO^{\bullet} + {}^{t}RH \longrightarrow {}^{t}BuOH + {}^{t}R^{\bullet} \quad (8)$$

$$^{t}R^{\bullet} + O_2 \longrightarrow {}^{t}RO_2^{\bullet} \quad (9)$$

$$^{t}RO_2^{\bullet} + {}^{t}RO_2^{\bullet} \longrightarrow {}^{t}ROOOOR^{t} \quad (10)$$

The selectivity of hydrogen abstraction by $^{t}BuO^{\bullet}$ ensures that tertiary peroxyls predominate over secondary and primary peroxyls.[13,14] The concentrations of these latter radicals are also low because of their rapid removal by irreversible termination reactions at temperatures below 155 K. As long as the temperature does not exceed 155 K, the peroxyl concentration can be changed consistently, and repeatedly, by cycling the temperature of the sample between 155 and 110 K without detectable loss of signal.

Injection of reactive substrates into the tetraoxide solutions

The reactions of substrates with peroxyls in equilibrium with their corresponding tetraoxides were studied by rapid *in situ* injection and mixing of cold substrate solutions into the tetraoxide equilibrated solutions contained in spectrosil tubes within the EPR cavity at low temperatures.

The magnetic field was set to the peak of the single line peroxyl EPR signal (g = 2.015) and the decay monitored continuously over several half-lives. The detailed procedure was as follows.

(i) An oxygenated solution of di-*tert*-butyl peroxide (7–10%) in 2MB of known volume was photolysed in spectrosil tubes held in an EPR cavity at ~200 K to obtain a steady state peroxyl concentration.

(ii) The temperature was lowered to a prescribed temperature, and the system allowed to re-equilibrate. The resonance position of the signal was located and the magnetic field set at this value. The spectrometer field scan was then set to zero.

(iii) With a stable peroxyl concentration established, a time scan was started and a chilled substrate solution of known concentration was rapidly injected directly into the tetraoxide equilibrium solution from a cold glass syringe *via* a stainless steel capillary outlet projecting below the surface of the solution (see below for the assessment of mixing times).

(iv) The weight of the final solution, and hence its volume, were determined at the end of the experiment. This, together with the known volume of the starting solution, allowed the initial peroxyl and substrate concentrations to be estimated.

Assessment of the mixing period

There is an inherent 'dead time' in the injection method since it takes time for the solutions to become homogenous and for the Q factor of the cavity to attain its new post-injection value. This 'mixing time' was estimated by injecting a known volume of neat 2MB solvent into the tetraoxide system and observing the time taken for the peroxyl concentration to level off (Fig 1). The mixing was complete within 35 s and thus all kinetic calculations were based on data accumulated after this 35 s period.

Results

Determination of the thermodynamic parameters of the tetraoxide–peroxyl equilibrium

Since no irreversible decay occurs below 155 K, the following mass balance equation is obtained ($[^{t}BuO_2^{\bullet}]_{max}$ is the peroxyl concentration at complete tetraoxide dissociation):

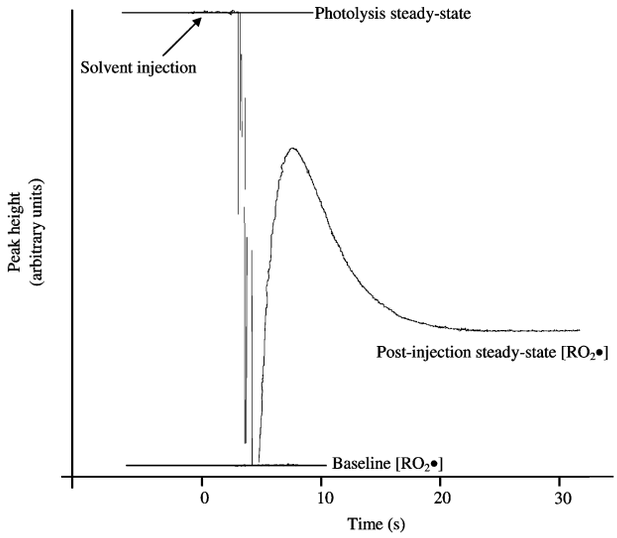

Fig. 1 Blank injection of 2MB into tetraoxide equilibrium at 130 K.

$$2[^{t}BuO_4Bu^{t}] + [^{t}BuO_2^{\bullet}] = [^{t}BuO_2^{\bullet}]_{max} \quad (11)$$

Substitution for the value of $[^{t}BuO_4Bu^{t}]$ together with the integrated van't Hoff isochore for K into eqn. (4) gives:

$$\ln\frac{[^{t}BuO_2^{\bullet}]_{max} - [^{t}BuO_2^{\bullet}]}{2} - 2\ln[^{t}BuO_2^{\bullet}] = \frac{\Delta S^{\circ}}{R} - \frac{\Delta H^{\circ}}{RT} \quad (12)$$

Rearrangement of eqn. (12) gives the more easily computed temperature relationship eqn. (13):

$$T = \frac{a}{\ln(b - [^{t}BuO_2^{\bullet}]) - 2\ln[^{t}BuO_2^{\bullet}] - \ln 2 + c} \quad (13)$$

$$Where\ a = -\frac{\Delta H}{R},\ b = [BuO_2^{\bullet}]_{max}\ and\ c = -\frac{\Delta S}{R}$$

This function is modelled by floating the variables $[BuO_2^{\bullet}]_{max}$, ΔH and ΔS, to obtain the best fit to the experimental $[^{t}BuO_2^{\bullet}]$ temperature profile (Fig 2). The values of ΔH and ΔS were established under our experimental conditions since they are used in determining the rate constants of peroxyl reactions with substrates.

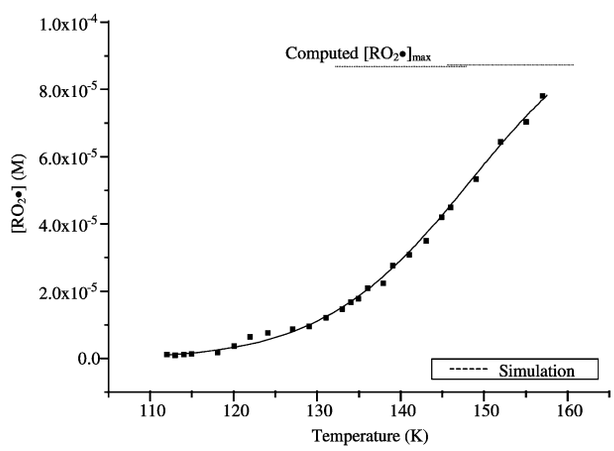

Fig. 2 The variation in peroxyl concentration with temperature from radicals produced by photolysis at 200 K and simulation.

In order to reduce the production and persistence of *tert*-alkyl methyl trioxide, the *tert*-alkyl tetraoxide was generated at

temperatures above 200 K to ensure that all cross-combined polyoxides were rapidly decomposed. This procedure provided a good fit between modelled and experimental $^tRO_2^\bullet$ profiles over a temperature range of 120–155 K. The estimated values of $\Delta H = 33 \pm 1$ kJ mol^{-1} and $\Delta S = 139 \pm 6$ J K^{-1} mol^{-1} compared favourably with those reported in the literature for different solvents, $\Delta H = 37 \pm 4$ kJ mol^{-1} and $\Delta S = 160 \pm 30$ J K^{-1} mol^{-1}.[9,10] No such correspondence was obtained from tetraoxides prepared below 200 K because the presence of trioxides perturbed the tetraoxide equilibrium.

The O–O bond energy in tetraoxides is ~33 kJ mol^{-1} while those in trioxides and peroxides are 80 and 120 kJ mol^{-1} respectively; there is progressive weakening of the bond with replacement of O–C bonds by O–O bonds. The change in entropy of ~130 J K^{-1} mol^{-1} is that expected for the loss of a translational degree of freedom when two particles combine. We have used the enthalpy and entropy values determined here for all kinetic analyses in order to minimise errors arising from variations in the experimental designs of different workers.

Mechanistic and kinetic studies of peroxyl and substrate reactions

All the peroxyl decays displayed the same characteristic of an initial, sharp peroxyl signal reduction during the mixing period followed by a slower decay resulting from the substrate peroxyl reactions.

Development of rate equations. We have used as substrates the two phenolic antioxidants, 2,6-di-*tert*-butyl-4-methylphenol (IONOL), and 2,4-dimethyl-6-*tert*-butylphenol (DMBP):

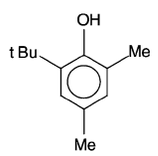

2,4-dimethyl-6-*tert*-butylphenol

DMBP

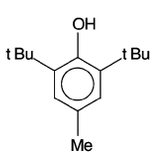

2,6-di-*tert*-butyl-4-methylphenol

IONOL

With these substrates reaction (14) [and possibly (15)] removes peroxyls:

$$^tBuO_2^\bullet + {}^tBuO_2^\bullet \underset{k_{-1}}{\overset{k_1}{\rightleftharpoons}} {}^tBuO_4Bu^t$$

$$RO_2^\bullet + AH \xrightarrow{k_2} ROOH + A^\bullet \quad (14)$$

$$A^\bullet + RO_2^\bullet \xrightarrow{k_3} AOOR \quad (15)$$

In the absence of the substrate AH:

$$\frac{d[RO_2^\bullet]}{dt} = 0 = k_{-1}[RO_4R] - 2k_1[RO_2^\bullet]^2 \quad (16)$$

In the presence of the substrate:

$$\frac{d[RO_2^\bullet]}{dt} = k_{-1}[RO_4R] - 2k_1[RO_2^\bullet]^2 - 2k_2[RO_2^\bullet][AH] \quad (17)$$

This equation can be treated at three levels of approximation.

First level approximation: when $[RO_2^\bullet]_0 \ll [AH]_0$. If the substrate reaction only causes a small perturbation of the equilibrium, *i.e.* $k_2[AH] \ll 2k_1[RO_2^\bullet]$, the algebraic sum of the first two terms of eqn. (17) will approximate to zero. A pseudo-first order logarithmic decay will result as long as [AH] remains substantially constant at its initial value $[AH]_0$.

$$\frac{d[RO_2^\bullet]}{dt} = -2k_2[RO_2^\bullet][AH]_0 \quad (18)$$

Integration gives,

$$\ln\frac{[RO_2^\bullet]_t}{[RO_2^\bullet]_0} = -2k_2[AH]_0 t \quad (19)$$

Linear plots of $\ln [RO_2^\bullet]_t$ *vs.* time were obtained when $[RO_2^\bullet]_0 \ll [AH]_0$. A typical first order plot is shown in Fig 3. The rate

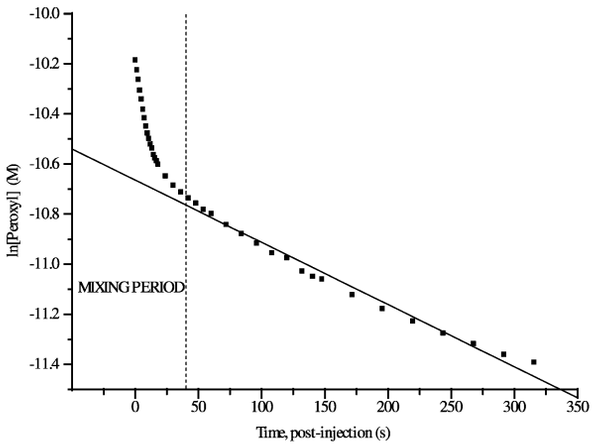

Fig. 3 *First level approximation* for IONOL injection (2.0×10^{-5} M) into the tetraoxide equilibrium at 140 K.

constants determined from the gradient were reasonably close to those estimated from literature values of the activation energy and frequency factors for the IONOL reaction.[15–17]

However, the condition imposes limitations on this rather approximate analysis. The second level of approximation includes the diminishing concentration of AH with time in the kinetic analysis.

Second level approximation: when $[AH]_0 \approx [RO_4R]$. When $[AH]_0$ and $[RO_2^\bullet] - [RO_4R]_0$ are comparable, eqn. (20) applies at all times after the mixing period:

$$\frac{d[RO_2^\bullet]_t}{dt} = -2k_2[RO_2^\bullet]_t[AH]_t \quad (20)$$

Mass balance considerations of oxygen and AH, and evaluation of standard integrals,[18] leads to two alternative analytical solutions dependant upon whether the value of the term q below is positive or negative:

$$q = 4ac - b^2 = 8K([AH]_0 - 2K[RO_2]_0^2 - [RO_2]_0) - 1$$

When $q > 0$ (the high antioxidant concentration, low temperature case):

$$-2\alpha k_2 t = 2\ln\left[\frac{x_t}{x_0}\right] - \ln\left[1 + \frac{2K(x_t^2 - x_0^2) + x_t - x_0}{2[AH]_0}\right] + \frac{2}{\sqrt{q}}\left[\tan^{-1}\frac{4Kx_0 + 1}{\sqrt{q}} - \tan^{-1}\frac{4Kx_t + 1}{\sqrt{q}}\right] \quad (21)$$

When $q < 0$ (the low antioxidant concentration, high temperature case):

$$-2\alpha k_2 t = 2\ln\left[\frac{x_t}{x_0}\right] - \ln\left[1 + \frac{2K(x_t^2 - x_0^2) + x_t - x_0}{2[AH]_0}\right] + \frac{1}{\sqrt{-q}}\left[\ln\frac{4Kx_0 + 1 - \sqrt{-q}}{4Kx_t + 1 - \sqrt{-q}} - \ln\frac{4Kx_0 + 1 + \sqrt{-q}}{4Kx_t + 1 + \sqrt{-q}}\right] \quad (22)$$

where $x = [RO_2^\bullet]_t$ *and* $\alpha = 2[AH]_0 - (2K[RO_2^\bullet]_0^2 + [RO_2^\bullet]_0)$.

The value k_2 can be estimated from the slope ($-2ak_2$) of the linear plots of the RHS of eqns. (21) or (22) *versus* time. A typical plot for DMBP is shown in Fig 4.

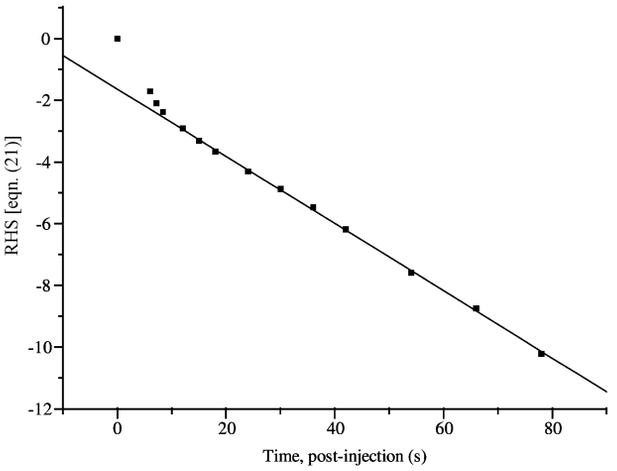

Fig. 4 *Second level approximation*: eqn. (21) plotted against time for DMBP injection into the tetraoxide equilibrium at 147 K. $[AH]_0 = 1.90 \times 10^{-4}$ M, $[RO_2^{\bullet}]_0 = 6.5 \times 10^{-5}$ M.

The second level approximation still makes the assumption of an unperturbed tetraoxide–peroxyl equilibrium. This was removed in the third refinement in which numerical computing kinetic modelling methods were used to solve the complete set of coupled differential equations that describe the $^tRO_2^{\bullet}$ decay profiles.

Third level approximation: kinetic modelling of the full reaction scheme. The numerical approach removes the assumptions that antioxidant (AH) levels are unchanging and that an unperturbed equilibrium exists. It therefore places more stringent tests on the reaction scheme, and provides more reliable kinetic parameters.

The initial test of the kinetic modelling reaction scheme used Kismet[19] computer software. The full numerical model (Scheme 1) was developed using Acuchem[20,21] which allowed

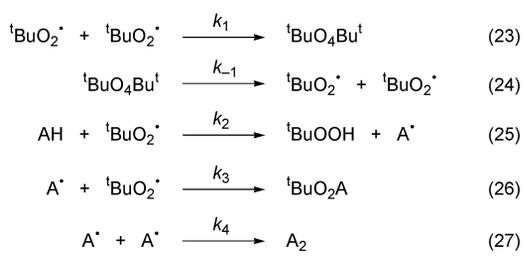

Where AH is an inhibited phenol.

Scheme 1 The mechanism used for simulation of peroxyl decay after antioxidant injection into the tetraoxide equilibrium.

values for $[RO_2^{\bullet}]_0$ and $[AH]_0$ to be inserted and the rate parameters floated to obtain the best fit between simulated and experimental peroxyl decay profiles.

Constraints are set on some of the rate constants and the reasonable assumption is made that the rate constants of radical–radical combination reactions, k_1, are near the diffusion limit, 10^8 M^{-1} s^{-1}.[22] The rate constant k_{-1} is equal to K/k_1.

The measured rate constants for disproportionation and combination for the phenoxyl radicals from IONOL range between 1×10^3–1.6×10^4 s^{-1} and 6.3×10^{-3}–2.0×10^{-2} M^{-1} s^{-1} respectively at 293–298 K.[23–25] We have used a value of 1×10^{-3} M^{-1} s^{-1} in our modelling. The contribution of these reactions is insignificant compared with the fast phenoxyl reaction with peroxyls to form cyclohexadienones ($k \approx 10^8$ M^{-1} s^{-1} at 197 K).[17] The level of $[A^{\bullet}]$ is thus low. In the absence of accurate Arrhenius parameters for this reaction we have adopted a value of 10^7 M^{-1} s^{-1} for both phenols.

Modelling procedure

The concentrations of $[RO_2^{\bullet}]_m$ and $[AH]_m$ at the end of the mixing period need to be estimated since both are less than those at $t = 0$, $[RO_2^{\bullet}]_0$ and $[AH]_0$. $[RO_2^{\bullet}]_m$ is given by the observed value of $[RO_2^{\bullet}]_t$ at $t = 35$ s, and $[AH]_m$ was calculated from the decrease of peroxyl levels in the following way:

$$\Delta[AH]_m = 2\Delta[RO_2^{\bullet}] = 2([RO_2^{\bullet}]_0 - [RO_2^{\bullet}]_m) \quad (28)$$

where $[RO_2^{\bullet}]_0$ is the observed steady-state value adjusted for dilution by the injected volume of substrate solution. Thus

$$[AH]_m = [AH]_0 - 2\Delta[RO_2^{\bullet}] \quad (29)$$

We assume a maximum of two peroxyls were lost by reaction with one molecule of inhibited phenol.

The rate parameters inserted as starting parameters into the numerical model are listed in Scheme 2. Typical simulated and experimental peroxyl decay profiles are shown in Figs. 5 and 6.

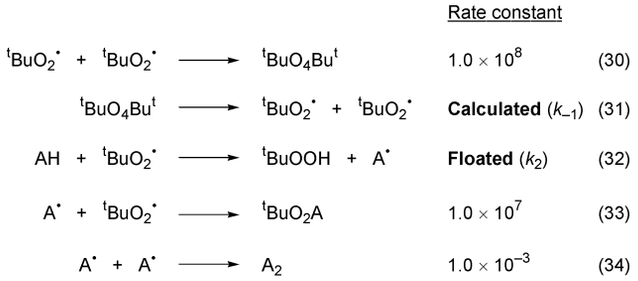

Scheme 2 Fixed rate constants inserted into the Acuchem model used for simulation of peroxyl decay after inhibited phenol injection into the *tert*-butylperoxyl–tetraoxide equilibrium.

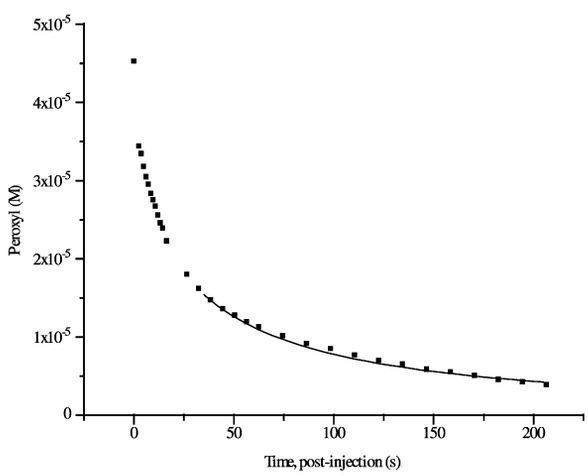

Fig. 5 Curve fitting of experimental data after IONOL injection (1.8×10^{-5} M) into the *tert*-butylperoxyl–*tert*-butyl tetraoxide equilibrium at 154 K.

The estimated values of the rate constant k_2 for hydrogen transfer reaction (32) give reasonably good Arrhenius plots for both IONOL and DMBP (Figs. 7 and 8).

The resulting Arrhenius parameters are collected together with those for the IONOL reaction determined by KEPR in Table 1. The present values are well within previous estimates even though we have been obtained data at much lower temperatures than previously used. No literature data exists for the direct comparison of k_2 at these low temperatures.

We also report the first measurements of the rate constant for the peroxyl reaction with DMBP at any temperature, although

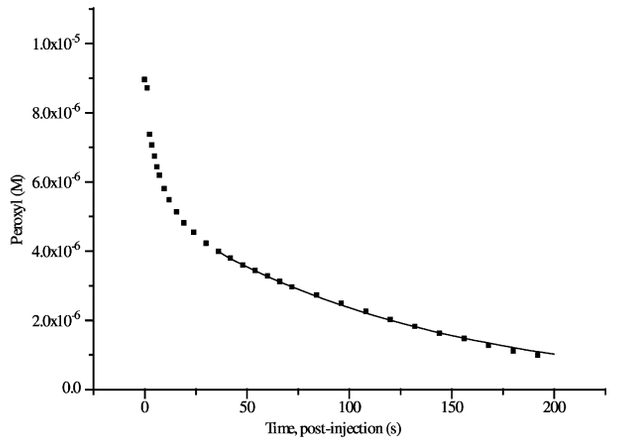

Fig. 6 Curve fitting of experimental data after DMBP injection (1.9×10^{-4} M) into the *tert*-butylperoxyl–*tert*-butyl tetraoxide equilibrium at 147 K.

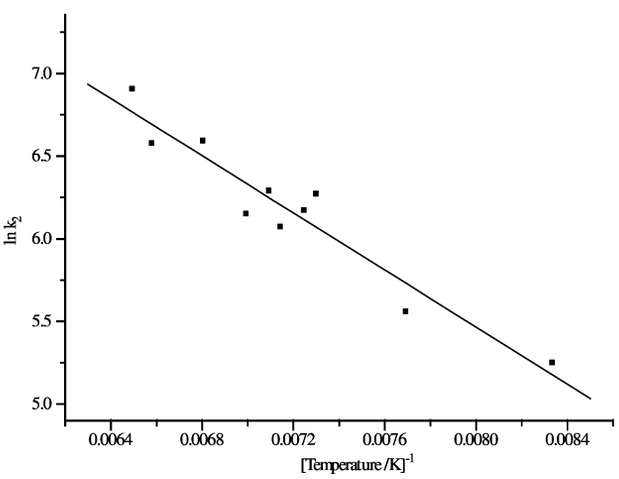

Fig. 7 Arrhenius plot for the *tert*-butylperoxyl reaction with IONOL.

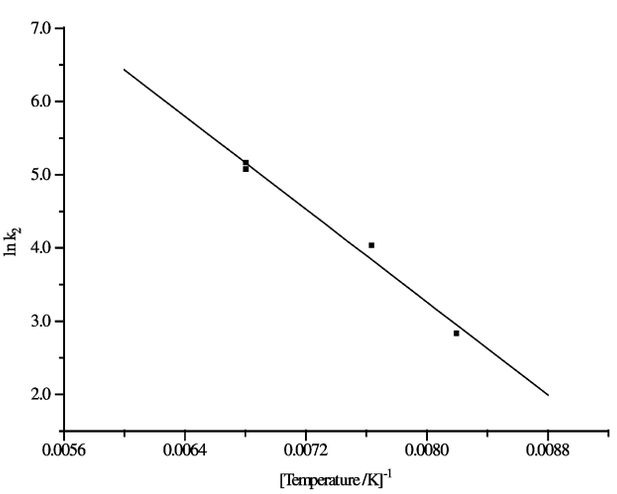

Fig. 8 Arrhenius plot for the *tert*-butylperoxyl reaction with DMBP.

rough estimates relative to the IONOL reaction can be made from the induction times for hydrocarbon autoxidation in the presence of the two antioxidants.

The values of k_2 at the higher temperatures used in previous studies were estimated from our measured Arrhenius parameters. These together with literature values are summarised in Table 2. The estimated k_2 shows a reasonable correlation with the rate constant measured by Howard.[17,26] The comparison with values obtained by Davies[15] and Bennett[16] at higher temperatures are less good, but are within a factor of 2. For this reason we conclude that the use of the tetraoxide equilibrium as a source of peroxyls at low temperatures provides a useful method for determining k_2 and gives reliable Arrhenius parameters which can be used to estimate antioxidant rate constants at the higher temperatures where hydrocarbon lubricants and antioxidants operate in practical applications.

Table 1 Arrhenius parameters for the peroxyl scavenging reaction (32) by injected inhibited phenols; literature comparisons are shown in italics

	T/K	E_a/kJ mol^{-1}	log (A/M^{-1} s^{-1})
IONOL	120–154	7.2 ± 0.8	5.4 ± 0.3
IONOL[17,26]	*183–303*	*3.36*	*4.6*
IONOL[16]	*253–312*	*9.35*	*5.6*
IONOL[15]	*192–311*	*7.1*	*5.14*
DMBP	122–147	13.2 ± 1.2	6.7 ± 0.5

Table 2 Literature values of k_2 for IONOL compared to extrapolated estimates using Arrhenius data from this study. Estimates for DMBP are shown in italics for comparison between phenols

		Estimated $k_2/10^3$ M^{-1} s^{-1}	
Temp./K	Literature $k_2/10^3$ M^{-1} s^{-1}	IONOL	*DMBP*
175	4.0[17,26]	1.8 ± 0.3	*0.58* ± 0.19
236	5.0[17,26]	6.4 ± 1.8	*6.0* ± 3.4
252	4.6,[15] 4.9[16]	8.1 ± 2.5	*9.3* ± 5.6
303	10.0[17,26]	14.4 ± 5.5	*27* ± 19

Comparison of k_2 for IONOL and DMBP

Although there are no measurements of the rate constants for the reaction of DMBP with peroxyls, the relative antioxidant efficiencies for a range of inhibited phenols are known. Scott[25,27] has reported the increased antioxidant effect of an *ortho* substituted α-branched alkyl and corresponding decrease in activity in the *para* analogue from his measurements of induction periods. Above ambient temperatures the reaction with DMBP is 1.7 times faster than that with IONOL.

At low temperatures we estimate the rates of peroxyl scavenging by DMBP to be slower than by IONOL. But our Arrhenius parameters give an extrapolated rate constant ratio at 303 K of 1.9, which is close to the estimate of Scott at this temperature. This arises because the reaction of peroxyl with DMBP has a higher activation energy.

Investigations of tertiary peroxyl and DMPO reactions using the tetraoxide equilibrium

5,5-Dimethyl-1-pyrroline *N*-oxide (DMPO), a cyclic nitrone, has found widespread use as a spin trap in circumstances where radical concentrations are too low for direct detection (Fig. 9).

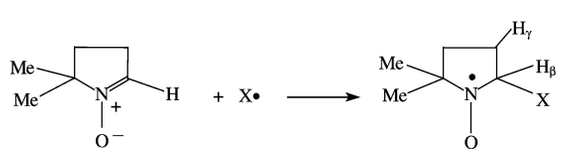

Fig. 9 The structure of DMPO.

The trap forms stable spin trap adducts at only one possible trapping site which accumulate to concentrations large enough for them to be seen by EPR. It is an efficient trap for thiyls[28–30] and alkoxyls[31–34] (rate constants of ~10^8 and 10^9 M^{-1}s^{-1} respectively at 298 K) and the primary radicals are well characterised in these cases.

However, identification of the trapped radical is a common problem in nitrone spin trapping and there is still controversy as to whether DMPO can actually trap peroxyls, except perhaps in exceptional circumstances.[35,36]

The clean source of tertiary peroxyls provided by the tetraoxide equilibrium should provide information about DMPO-peroxyl radical reactions. We have briefly reported our results in a previous paper [12] and present a fuller account here.

DTBP in 2MB (10% v/v) was photolysed at 200 K until a steady state peroxyl concentration was achieved (~5×10^{-5} M) after approximately 120 s. The temperature of this equilibrium solution held in the EPR cavity was then lowered to below 155 K and cold solutions of the DMPO (~10^{-3} to 10^{-4} M) were injected in the way already described.

The most surprising result, which was repeated several times, was that although the *tert*-peroxyl signal was rapidly, and completely, removed by the addition of DMPO ($t_{½}$ < 1 s), the peroxyl signal was not replaced by the expected EPR spectrum of a spin-adduct. Hence there is a total loss of paramagnetism and radicals from the solution at low temperature, indicating the formation of a diamagnetic complex between the DMPO and peroxyls.

The peroxyl signal disappeared virtually instantaneously on injection of the spin trap between 150 and 130 K. However, when this low temperature solution was warmed to 200 K, the characteristic spectrum of the alkoxyl adduct DMPO–OR was observed, but at much reduced intensity compared with the initial peroxyl level. Similar decompositions of a superoxide and alkylperoxyl DMPO complex to yield a hydroxide radical and the *tert*-butoxyl adducts respectively have been reported previously by Finkelstein *et al.*[37]

Davies *et al.*[35] claim to have observed a *tert*-butyl peroxyl DMPO adduct on photolysis of unusually high concentrations of *tert*-butyl hydroperoxide (800 mM) and DMPO (50 mM) in de-oxygenated toluene at room temperature. However, recently Dikalov and Mason [38] have used ^{17}O to show that only methoxy DMPO spin adducts are observed from methyl peroxyls with no trace of the corresponding methylperoxyl adduct. Our observations of no mono-tertiary alkyl DMPO spin adduct formation are in accord with these definitive results.

It appears that the DMPO does efficiently scavenge *tert*-alkylperoxyls at low temperatures but to form a diamagnetic product not a stable paramagnetic peroxyl DMPO spin adduct. We suggest that this loss of free spins probably arises by DMPO removing two peroxyls of opposite spins either concertedly or by rapid reaction of the monoperoxyl spin adduct with another peroxyl. The possibility that the monospin adducts decay rapidly by self termination can be discounted because the rate constants for such reactions are very low and indeed the persistence of spin adducts, and the absence of significant self terminations, are the basis for their use. The decay of the peroxyls on introduction of DMPO (10^{-3}–10^{-4} M) occurred in less than one second, so that the rate constant for the second order reaction must be greater than 10^3–10^4 M^{-1} s^{-1}.

The most likely diamagnetic product is that where two peroxyls have been scavenged by one DMPO molecule. We cannot ascertain from our EPR studies whether the proposed DMPO–diperoxyl peroxyl complex exists and decomposes thermally at higher temperatures to give an alkoxyl DMPO spin adduct [eqn. (35)]. Other techniques such as low temperature

$$\underset{\text{Non-paramagnetic}}{[\text{DMPO(OOR)}_x]} \rightarrow\rightarrow \underset{\text{Paramagnetic}}{\text{DMPO-OR}} \qquad (35)$$

IR, UV, and NMR need to be deployed to investigate this aspect further.

Conclusions

1. In the temperature range 110 to 155 K *tert*-alkylperoxyls are in a dynamic equilibrium with the corresponding di-*tert*-alkyl tetraoxide molecules. The concentration of peroxyls is readily measured by EPR and depends solely on the initial concentrations of tetraoxide and on temperature.

2. The combination of the peroxyls and the reverse dissociation of the tetraoxide both occur rapidly, so that the concentration of peroxyls can be recycled reversibly and indefinitely without loss by cycling the temperature between 110 and 155 K.

3. Such a stable concentration of *tert*-alkylperoxyls provides a very clean reliable source of these radicals in the absence of any other radicals.

4. By rapid injection and mixing of cold solutions of reactive substrates into solutions containing stable concentrations of peroxyls, mechanistic and kinetic information can be obtained about peroxyl–substrate reactions.

5. Injection of the phenolic antioxidants IONOL and DMBP results in a readily monitored decay of the peroxyl EPR signal. Three levels of approximation have been used to process the decay profiles to obtain rate constants and Arrhenius parameters for the peroxyl antioxidant hydrogen transfer reaction.

6. The most reliable results are those obtained by kinetic modelling of the total reaction scheme using numerical computing methods to solve the resulting set of coupled differential equations.

7. The rate constants and Arrhenius parameters derived by the tetraoxide method accord well with literature values for IONOL.

8. When the much used spin trap DMPO was added to an equilibrated peroxyl–tetraoxide solution between 130 and 150 K the single line peroxyl EPR signal decayed instantly to zero (half life < 1 s). But, surprisingly, the lost signal was not replaced by the expected multi-line spectrum of a paramagnetic spin adduct. However, on heating to 200 K a stable low intensity spectrum of the alkoxyl DMPO spin adduct slowly developed. This suggests that mono-peroxyl–DMPO spin adducts are not formed as has been suggested previously. We speculate that the DMPO reacts with two peroxyls of opposite spin either simultaneously or consecutively to form a diamagnetic adduct which decomposes to the alkoxyl spin adduct at higher temperatures.

9. With the simple injection method data is lost during the mixing time. Rapid mixing techniques, such as stopped flow, would reduce this dead time but these have technical difficulties because of the low temperatures required.

Acknowledgements

J. D. H. thanks the EPSRC for the award of a CASE studentship. Both authors are grateful to Shell Research Ltd for their contribution, support and interest.

References

1 N. A. Milas and S. M. Djokic, *J. Am. Chem. Soc.*, 1962, **84**, 3098.
2 P. D. Bartlett and T. G. Traylor, *J. Am. Chem. Soc.*, 1963, **85**, 2407.
3 J. R. Thomas, *J. Am. Chem. Soc.*, 1965, **87**, 3935.
4 P. D. Bartlett and P. Gunther, *J. Am. Chem. Soc.*, 1966, **88**, 3288.
5 N. A. Milas and B. Plesnicar, *J. Am. Chem. Soc.*, 1968, **90**, 4450.
6 S. W. Benson and J. H. Buss, *J. Chem. Phys.*, 1958, **29**, 546.
7 S. W. Benson, *J. Am. Chem. Soc.*, 1964, **86**, 3922.
8 P. D. Bartlett and G. Guaraldi, *J. Am. Chem. Soc.*, 1967, **89**, 4799.
9 J. E. Bennett, D. M. Brown and B. Mile, *Chem. Commun.*, 1969, 504.
10 K. Adamic, J. A. Howard and K. U. Ingold, *Chem. Commun.*, 1969, 505.
11 J. E. Bennett, D. M. Brown and B. Mile, *Trans. Faraday Soc.*, 1970, **66**, 397.
12 J. D. Honeywill and B. Mile, *Magn. Reson. Chem.*, 2000, **38**, 423.
13 C. Walling and B. B. Jacknow, *J. Am. Chem. Soc.*, 1960, **82**, 6108.
14 C. Walling and W. Thaler, *J. Am. Chem. Soc.*, 1961, **83**, 3877.
15 C. Davies, PhD thesis, UWCC, 1993.
16 J. E. Bennett, personal communication.
17 J. A. Howard, *Rev. Chem. Int.*, 1984, **5**, 1.
18 *Handbook of Chemistry and Physics*, ed. R. C. Weast, CRC Press, Cleveland, 1974.
19 *Kismet*, Shell Research Ltd, unpublished work.

20 W. Braun, J. T. Herron and D. K. Kahaner, *Int. J. Chem. Kinet.*, 1988, **20**, 51.
21 P. Neta, R. E. Huie, P. Maruthamuthu and S. Steenken, *J. Phys. Chem.*, 1989, **93**, 7654.
22 P. D. Sillman, B. Mile, A. Holmes and C. C. Rowlands, *J. Chem. Soc., Perkin Trans. 2.*, 1993, 2141.
23 S. A. Weiner and L. R. Mahoney, *J. Am. Chem. Soc.*, 1972, **94**, 1412.
24 R. D. Parnell and K. E. Russell, *J. Chem. Soc, Perkin Trans. 2.*, 1974, 161.
25 G. Scott, *Atmospheric Oxidation and Antioxidants*, Elsevier, Amsterdam, 1965.
26 J. A. Howard, *Rubber Chem. Technol.*, 1974, **47**, 976.
27 G. Scott, *Chem. Ind. (London)*, 1963, **41**, 271.
28 P. D. Josephy, D. Rehorek and E. G. Janzen, *Tetrahedron Lett.*, 1984, **25**, 1685.
29 M. J. Davies, L. G. Forni and S. L. Shuker, *Chem. Biol. Interact.*, 1987, **61**, 177.
30 B. Mile, C. C. Rowlands, P. D. Sillman and M. Fildes, *J. Chem. Soc., Perkin Trans. 2.*, 1992, 1431.
31 E. G. Janzen and C. A. Evans, *J. Am. Chem. Soc.*, 1973, **95**, 8205.
32 D. L. Haire and E. G. Janzen, *Can. J. Chem.*, 1982, **60**, 1514.
33 G. R. Buettner, *Free Radical Biol. Med.*, 1987, **3**, 259.
34 D. L. Haire, U. M. Oehler, H. D. Goldman, R. L. Dudley and E. G. Janzen, *Can. J. Chem.*, 1988, **66**, 2395.
35 M. J. Davies and T. F. Slater, *J. Biochem.*, 1986, **240**, 789.
36 P. Tordo, *Spec. Period. Rep. Electron Spin Reson.*, 1999, **2**, 16118.
37 E. Finkelstein, G. M. Rosen and E. J. Rauckman, *J. Am. Chem. Soc.*, 1980, **102**, 4994.
38 S. I. Dikalov and R. P. Mason, *Free Radical Biol. Med.*, 1999, **27**, 864.